

Gas Foil Bearing Coating Behavior in Environments Relevant to S-CO₂ Power System Turbomachinery

M.S. Walker, D. D. Fleming, and J. J. Pasch
Sandia National Laboratories
Livermore, CA USA



Dr. Matthew Walker (mswalke@sandia.gov) is a Senior Member of the Technical Staff at Sandia National Laboratories California. He specializes in the interaction of materials with their environment and with other materials at high temperature. His current research interest is focused on the evaluation of structural alloys for use in advanced energy systems. Most prominent among these are evaluating alloy performance in supercritical CO₂, which cuts across a range of energy technologies including nuclear, fossil, as well as renewable. Prior to joining Sandia, he worked for 5 years as a Materials Scientist at the Alcoa research center in Pittsburgh, PA. While at Alcoa, he developed ceramic and metallic materials for operation within the aggressive environments of molten fluoride salt as well as in molten aluminum. Before joining Alcoa, he received a MS and PhD in Materials Science and Engineering at Carnegie Mellon University.



Mr. Darryn Fleming is a Senior Member of Technical Staff focused on engineering large scale experiments ranging from 20 MWth steam test facilities to highly complex S-CO₂ power conversion cycles. Mr. Fleming is the Principal Investigator on several projects pertaining to the development of Supercritical CO₂ power cycles which include scaling studies to reach a 10 MW unit along with US manufactured and US exportable advanced Printed Circuit Heat Exchangers.



Dr. Jim Pasch has professional experience in four distinct fields. In 1995, he supported the Air Force Air Combat Training Systems program as a systems engineer in Fort Walton Beach, Florida. In 1998, Pratt & Whitney hired Jim as a member of their rocket propulsion systems team in West Palm Beach, Florida. Jim spent eight years in this capacity analyzing test and flight data from the Space Shuttle Main Engine. Jacobs Engineering hired Jim in 2006 as NASA ramped up the Constellation program to replace the aging shuttle fleet. While working at Marshall Space Flight Center, Jim was tasked with analyzing and quantifying various thermal hydraulic and control risks to the successful launch of the Ares I-X mission. In 2010, Sandia National Labs hired Jim for his thermodynamic and thermal hydraulic expertise, first to support the nuclear waste disposal program in Carlsbad, New Mexico, then to take over as the principal investigator for Sandia closed Brayton cycle R&D efforts in Albuquerque.

ABSTRACT

The Sandia S-CO₂ Recompression Closed Brayton Cycle (RCBC) utilizes a series of gas foil bearings in its turbine-alternator-compressors. At high shaft rotational speed these bearings allow the shaft to ride on a cushion of air. Conversely, during startup and shutdown, the shaft rides along the foil bearing surface. Low-friction coatings are used on bearing surfaces in order to facilitate rotation during these periods. An

experimental program was initiated to elucidate the behavior of coated bearing foils in the harsh environments of this system. A test configuration was developed enabling long duration exposure tests, followed by a range of analyses relevant to their performance in a bearing. This paper provides a detailed overview of this work. The results contained herein provide valuable information in selecting appropriate coatings for more advanced future bearing-rig tests at the newly established test facility in Sandia-NM as well as in other facilities that may exist for these types of tests.

1. INTRODUCTION

The supercritical carbon dioxide (S-CO₂) Brayton Cycle has gained significant attention in the last decade as an advanced power cycle capable of achieving high efficiency power conversion; it represents a thermal to electric energy conversion system with an efficiency approaching 50% under the operating conditions required for advanced energy systems. Sandia National Laboratories, with support from the U.S. Department of Energy Office of Nuclear Energy (US DOE-NE), has been conducting research and development in order to deliver a Recompression Closed Brayton Cycle (RCBC) that is ready for commercialization. There are a wide range of materials related challenges that must be overcome for the success of this technology. At Sandia, an area of recent focus has been on identifying the behavior of the coating materials used on gas foil bearings in the CO₂ environments relevant to these systems. At high shaft rotational speed these bearings allow the shaft to ride on a cushion of air. Conversely, during startup and shutdown, the shaft rides along the foil bearing surface. Low-friction coatings are used on bearing surfaces in order to facilitate rotation during these periods.

Through discussions with several of the companies that design and manufacture these types of bearings (Xdot Engineering and Analysis, Mechanical Solutions, and Mohawk Innovative Technology) it was realized that very little is known about the chemical compatibility of these coating materials with CO₂. Moreover, nothing is known about their behavior in CO₂ at conditions (pressure and temperatures) relevant to their application in an actual S-CO₂ bearing. It is of critical importance to understand the coating chemical behavior independent of mechanical loads. An experimental program was initiated to elucidate the behavior of coated bearing foils in the harsh environments of this system. A test configuration was developed enabling long duration exposure tests, followed by a range of analyses relevant to their performance in a bearing. This paper provides a detailed overview of this work. The results contained herein provide valuable information in selecting appropriate coatings for more advanced future bearing-rig tests at the newly established test facility in Sandia-NM as well as in other facilities that may exist for these types of tests.

2. BACKGROUND

2.1. Bearings for S-CO₂ Power Systems

In a general sense, a bearing is an element or assembly that guides or positions components subject to relative motion. For turbomachinery bearings, continuous rotation is required, and bearings are often classified as radial (journal) or axial (thrust) bearings. These are illustrated graphically in Figure 1, where the name of each derives from the positioning requirement. The fundamental requirement of a bearing is that it maintains the desired relative position, despite the forces or loads that must be transmitted. As such, it is important to minimize the wear which may be created by these surfaces under relative motion and load, and desirable to reduce the parasitic energy losses which invariably accompany bearings.

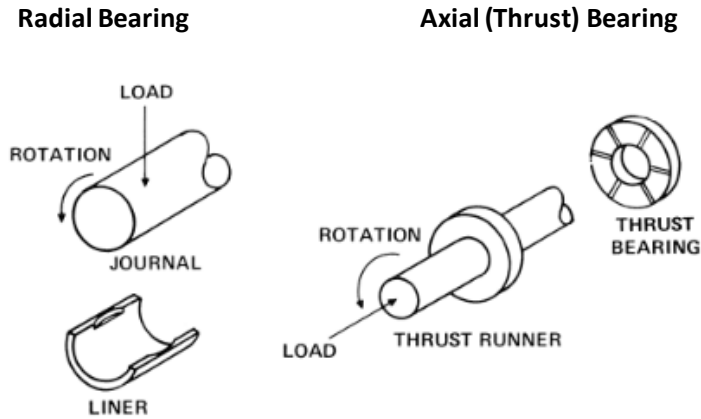


Figure 1. Two Main Categories of Continuous Rotation Bearings ^[1]

Turbomachinery for S-CO₂ power systems presents unique challenges to bearing support systems resulting from the working fluid properties of S-CO₂. It has significantly higher fluid density and lower viscosity than conventional working fluids. This combination results in compact, power-dense, turbomachinery which presents unique challenges relating to bearing surface speed and bearing unit load.

A variety of bearing types can be considered for S-CO₂ systems. A summary of the different bearing types considered for use in S-CO₂ applications and their relevant power ranges is given in Figure 2. The ones most commonly considered are ^[3]:

- (1) Gas Foil Bearings
- (2) Magnetic Bearings
- (3) Hydrostatic (CO₂ Liquid or Gas) Bearings
- (4) Hydrodynamic (CO₂ Liquid or Supercritical Fluid) Bearings
- (5) Hydrodynamic (Oil Lubricated Tilt-Pad) Bearings
- (6) Hydrodynamic (Oil Lubricated Roller or Elliptical) Bearings

Large industrial sized power plants rely primarily on hydrodynamic oil tilting pad bearings for both the thrust and journal loads. Some consider these the most likely candidate for future large scale S-CO₂ systems ^[2,3]. The advantages that they have over the others for future S-CO₂ technology, is that they are commercially available from a variety of OEMs, they are rotor dynamically stable, able to withstand high axial and radial loads, and can operate at shaft speeds up to 30,000-40,000 rpm on the small-diameter shafts needed for pilot plants in the 10MW_e power range. The use of these bearings in S-CO₂ systems leverages the significant industrial investment in this technology, and confirms that standard industrial seals and buffer gas management systems can be used with minimal loss in this application.

The other bearing types (gas foil bearings, magnetic bearings, hydrostatic bearings, and hybrid bearings) are useful primarily for S-CO₂ R&D test facilities. These offer potential advantages that include simplified sealing systems, higher operating speeds, and longer shafts by placing the bearing midway along the length of a multi-staged turbomachine. Disadvantages with these include design challenges such as complicated rotor dynamics, high windage, and heating with requirements for local cooling. An additional disadvantage is the lack of history with these bearings in the power industry, whereas there is a long history with the oil bearings.

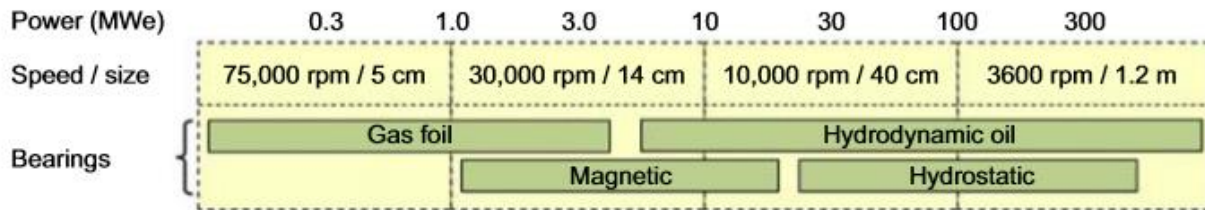


Figure 2. Types of bearings proposed for use in S-CO₂ applications across range of rotor power [2]

The landscape of S-CO₂ power systems development includes the development and use of a variety of these bearing approaches. Research teams in Korea (KAIST [4] and KIER [5]) used gas foil bearings in a 100kWe test loop, oil lubricated tilt-pad bearings in a 80kWe system, and magnetic bearings in a turbopump. For the GE/SWRI collaboration under the SunShot program, oil lubricated tilt-pad journal bearings were used in their 10MWe prototype system [2]. Barber-Nichols has advocated for the use of S-CO₂ hydrostatic bearings as an alternative to traditional hydrodynamic bearings [6]. They describe the performance of S-CO₂ hydrostatic bearings exceeding most other bearing technologies in load capacity, stiffness, and damping. The principal disadvantages for these are their cost, complexity, and inefficiency of using an external supply. Companies that design and build bearings have described ongoing work to develop porous externally pressurized gas bearings [7] and advanced gas foil bearings [3] for S-CO₂ turbomachinery. For the 250kWe S-CO₂ test system at Sandia, gas foil bearings were developed for both radial and thrust support [8]. More details for the bearing technology used in this system is described in the next section of this report.

2.2. Gas Foil Bearings

Key attributes to gas foil bearings are that they are oil-free, compact, lightweight, and tolerant of high frequency-low displacement loads. Various designs for radial and thrust gas foil bearings exist. These include bump type, leaf type, and tape type. In each case the spinning shaft is supported on a thin film of air or process gas. No oil sealing or liquid lubrication is required. Due to there being no spinning parts to the bearing, they are well suited to high shaft speeds. With the elimination of lubrication, they are good for both low and high temperature operation. Furthermore, due to their flexible structure, they can tolerate significant shock loads, as well as substantial misalignment and dust/debris.

Among the three type of gas foil bearings, the bump type has been the most popular. It is comprised of three basic components: a smooth top foil, a corrugated bottom foil or “bump foil”, and the support structure, usually a cylindrical shell for journal bearings and a flat disc for thrust bearings. Illustrations for these bump type foils are shown in Figure 3. Both the top and bottom foils are made from thin sheets of compliant metal, typically a nickel-based alloy such as Inconel X750. In a typical configuration, the top foil is affixed to the bearing housing at a point, and is initially allowed to sit to the height of its bump understructure. During loading and running, the foils are perturbed by the film pressure profile and resultant deflection of the foil bearing.

For normal, steady-state operation of these bearings, the shaft is supported on a fluid film, eliminating contact between the shaft and bearing. Conversely, at lower speeds during startup and shutdown, the shaft rides along the foil itself. To extend the life of the bearings and also to facilitate rotation during these periods, coatings are applied to the top foil, the shaft journal, or both to minimize friction and wear. Important requirements for these surface coatings include chemical compatibility with the fluid environment, surface properties (surface roughness, coefficient of friction, etc.) to minimize abrasive wear and particle debris generation, and good adhesion to the metal substrate.

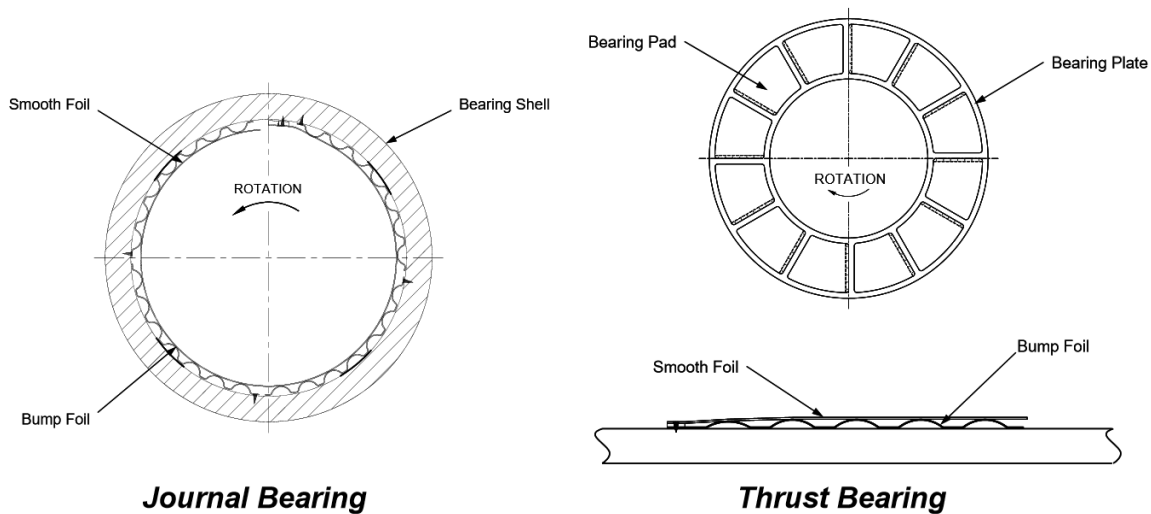


Figure 3. Typical construction for bump foil journal and thrust bearings [3]

2.3. Sandia RCBC System

The Sandia S-CO₂ RCBC loop Turbine-Alternator-Compressor (TAC) was developed utilizing a series of gas foil bearings. Radial (or Journal) bearings are located at both the turbine and compressor sides of the TAC, while the compressor side also has an axial (or thrust) bearing. Each bearing operates in an environment of around 300 psi CO₂. The turbine-side radial bearing is at a significantly higher temperature (~ 550°C) than at either of the compressor-side bearings (~ 315°C). The locations for each bearing are shown in Figure 4.

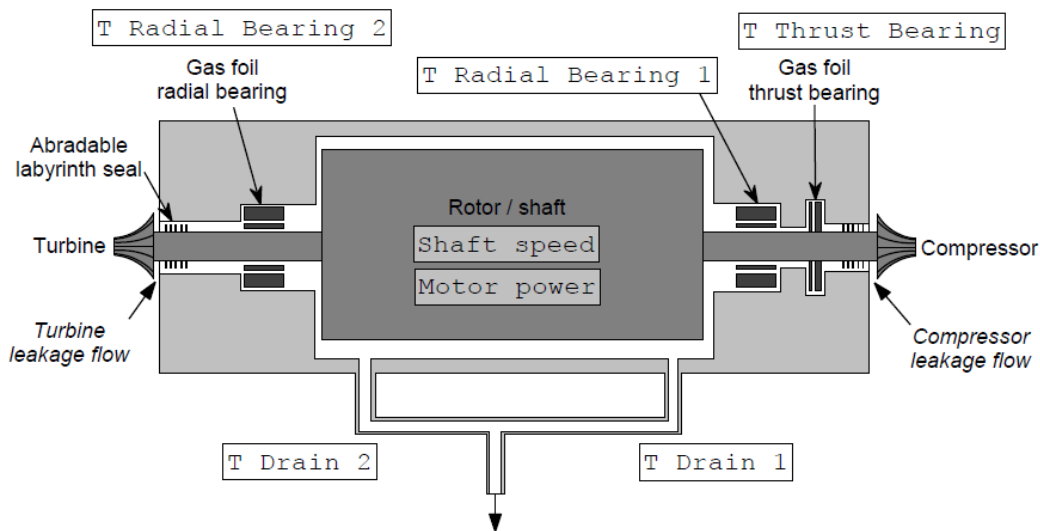


Figure 4. Diagram of Sandia's S-CO₂ TAC showing the location for the bearings

The journal bearings were obtained off-the-shelf from Capstone. These are approximately 2" long and 1.5" in diameter and have different solid lubricant coatings for the turbine and compressor sides of the TAC. The high temperature turbine side journal bearing uses a patented Capstone coating material with an upper temperature limit of 538°C (1000°F), while the compressor end journal bearing uses a Teflon-based coating capable of reaching temperatures of 232°C (450°F). In both cases the foil themselves are

made from Inconel X750. No commercial manufacturer was identified to deliver a foil thrust bearing, therefore they were designed and built in-house at Barber-Nichols from open source information provided by NASA Glenn Research Center. Based on NASA's experience, a foil thrust bearing was developed which was 4" outer diameter, 2" internal diameter, and featured 6 pads. The foils themselves were made from Inconel X750, and a Teflon coating was applied as the foil coating material.

Information regarding the performance of gas foil bearings has been gleaned through their short duration operation in the Sandia S-CO₂ RCBC during the past several years. The journal bearings have appeared to work adequately; while there have been significant challenges with the thrust bearings. In fact, thrust bearings have been identified as a limiting issue in S-CO₂ turbomachinery development for small-scale hardware^[8]. Consensus is that the Teflon coating appears inadequate for the temperatures in which this bearing operates, and there is a need for hardware that is capable of sustaining higher temperatures during operation. While the journal bearings have appeared to work well, they have challenges of a different nature. The company that makes these, Capstone, no longer sells their journal bearings. An alternative source for journal bearings is currently needed, with the complication of not knowing the high temperature coating material that Capstone was using on their versions of turbine-side journal bearings.

Collectively, these issues prompted the need to initiate an investigation to evaluate and identify alternative foil coating materials for these bearings. Very little is actually known about the behavior of foil coating materials in the high temperature/pressure CO₂ environment of these bearings, and there is tremendous value to obtaining this information in a manner independent of mechanical loads.

3. EXPERIMENTAL APPROACH

An experimental program was initiated to elucidate the behavior of coated bearing foil materials in the harsh environments of the Sandia RCBC system. The overall approach to this work involved the following main activities: (1) Collaborating with gas foil bearing vendors to identify candidate foil coating materials to be tested, (2) Acquiring samples of the various coating materials in formats relevant to use in an actual RCBC system, (3) Developing an appropriate test configuration for completing the evaluations, (4) Identifying appropriate sample characterizations that are relevant to coating material performance within a gas foil bearing, and (5) Completing a series of long duration exposure tests (500hr) along with the appropriate post-test sample characterizations. Details are provided in each of these areas in this section of the paper.

3.1. Identification of Candidate Foil Coating Materials

The starting point for conversations with gas foil bearing vendors regarding foil coating materials, was the operating environment (pressure and temperature) for the various bearings within the TAC. Analysis by members of the Sandia S-CO₂ team in Albuquerque, NM established a pressure of 300 psi CO₂ at both the turbine-side and compressor-side bearings. Additionally, a temperature of 550°C was established for the turbine-side bearings, and a temperature of 315°C was established for the compressor-side. Using this information, bearing vendors were able to identify a variety of candidate materials for these evaluations. In some instances, candidate materials were identified to be evaluated at only one of these two conditions (315°C or 550°C), while in others materials were identified to be evaluated at both.

Three vendors were approached to collaborate on this project: (1) Xdot Engineering and Analysis of Charlottesville, VA, (2) Mechanical Solutions of Albany, NY, and (3) Mohawk Innovative Technology of Albany, NY. Two of these vendors, Mohawk Innovative Technologies and Mechanical Solutions, Inc.,

expressed concern over the public release of their coating chemical formulation associated with the analyses as part of this program. An NDA was established with Mechanical Solutions, Inc., that will protect their coating chemical formulation from public release. In the case of Xdot, they differ a bit from the others, as they are more focused on bearing design rather than on developing coating materials themselves.

Besides evaluations of newly identified coating materials, inclusion of samples that have the current coatings used in Sandia's test loop bearings is important as a comparison. This establishes a baseline of performance, against which to compare the other options being evaluated. Unfortunately, only samples with the low temperature compressor-side thrust bearing coating were included, as the supplier for the other bearings (Capstone Turbines) was unwilling to provide samples for these tests.

3.1.1. Xdot Engineering and Analysis

Xdot worked with four separate coating vendors to provide a series of 6 different coatings for evaluation. Being involved in bearing design, it was very important to Xdot that the coating be evaluated in the format that it will be used in a real bearing. To achieve this, they provided samples for each of the coatings across a range of possible formats. The different sample formats included flat foil, rolled or curved foil, and cylindrical; these are shown in Figure 5. In each case the coating material was applied to the sample surface. The flat foils were included to represent the thrust bearing foils, while the curved foils represent those for the journal bearing. The cylindrical samples represent a case where the coating is applied to the rotating shaft itself rather than to the bearing foils.

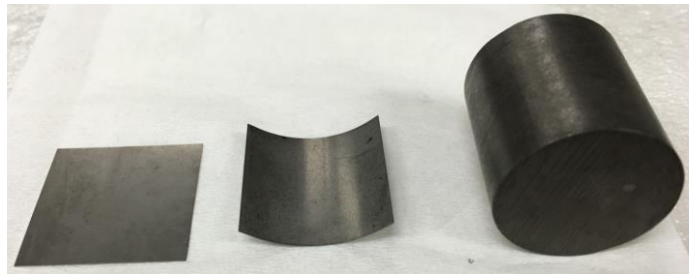


Figure 5. Sample formats used for gas foil bearing performance evaluations

One of the coating vendors was Everlube Products (Peachtree City, GA), which is a business unit of Curtiss-Wright. Two of their solid film lubricant materials, Perma-Slik RMAC and RWAC, were evaluated at both of the exposure conditions in both the flat foil and curved foil sample formats. The foil substrate material for these samples was 1" x 1" Inconel X750. The RMAC product uses molybdenum disulfide (MoS_2) as the solid lubricant, while the RWAC product uses tungsten disulfide (WS_2).

A second coating vendor was General Magnaplate (Linden, NJ). Two of their Nedox 10K coatings, 10K2 and 10K3, were evaluated in both the flat foil and curved foil sample formats. The foil substrate material for these samples was 1" x 1" Inconel X750. The 10K2 material was evaluated only at the higher temperature exposure condition, while the 10K3 was evaluated only at the lower temperature condition. Both materials appear to use primarily nickel in the coating.

TURBOCAM International (Dover, NH) was a third coating vendor. Their TX1 surface treatment differed versus all of the other materials investigated, as this was not a coating, but rather a metal surface treatment process (nitride) imposed on the surface. Here, the presence of nitrogen at the sample surface imparts hardness, wear resistance, and lubricity to the surface. TX1 was evaluated at both of the exposure

conditions in all three sample formats. The substrate material was now 1" x 1" 316 stainless steel rather than Inconel X750, due to the requirements for the surface treatment process. For both the flat and curved foil samples, samples were evaluated for three separate vendor applications of the surface treatment. These samples are designated as treatments A, B, and C, and the parameters of the surface treatment process differed slightly among the three.

A final coating was the NASA developed PS400 material, which is provided by Hohman Plating and Manufacturing (Dayton, OH). This material, being applied to the metal surface by plasma spray, was provided onto thicker metal substrates (0.125") of 1.25" x 1.25" 15-5 stainless steel. In an actual bearing application, it would likely be applied to the thrust runner disk surface or shaft, rather than to the bearing foils. It was evaluated in this thicker plate format at both of the exposure conditions. PS400 is the latest in a long line of plasma-sprayed solid lubricant coatings dating back to the 1970s, all developed at NASA Glenn Research Center ^[9,10]. It is comprised of a nickel-molybdenum-aluminum binder with added chromium oxide, silver, and barium-calcium fluoride. The silver and barium-calcium-fluoride (5% by mass) provide the solid lubrication, while chromium oxide (25%) is used as a hardener, and nickel-moly-aluminum (70%) is tough binder matrix to stabilize the solid layer. Compared to the previous generation coating PS304, it has higher density, smoother finish, better stability, good creep resistance, strength, oxidative and dimensional stability. Solid lubricant content was halved from 10wt% to 5 for PS400 as compared to its predecessor. Total coating thickness of at least 300 μm, is built up layer by layer in many separate plasma spray passes.

3.1.2. Mechanical Solutions

It is unclear if Mechanical Solutions worked with a coating vendor to develop their gas foil bearing coating materials, or whether they have developed these internally. They did not provide any information on their coating materials, as this is a sensitive technology to their business that they would like to protect. The chemistry of their coating materials will not be disclosed as part of this report, but instead the performance of these materials will be compared to the others included in this study.

Samples with three different coating materials were provided for these evaluations; these were labeled by the vendor as A39, A40, and A42. The differences between these three materials were not disclosed, and so these will be treated separately as three separate coating options. These were provided in the 1" x 1" flat foil format only, and the substrate material was Inconel X750. All of the samples were evaluated at both sets of exposure conditions.

3.2. Exposure Furnace Setup

The test configuration for these evaluations was established using the high temperature autoclave furnace that was used previously for the carbon steel S-CO₂ corrosion study ^[11]; this is located at the laboratory in Livermore, CA. The furnace itself was modified to allow for tests in a controlled atmosphere of 300 psi CO₂, instead of in S-CO₂. While the pressure is maintained at 300 psi, the setup allows for a flow of fresh CO₂ through its chamber. Temperature of the internal chamber is measured across its length in three locations. A photo of the furnace setup for these tests is shown in Figure 6.

A new sample holder approach was designed for use in these experiments. This was an important aspect to this work, as there were many different sample types and formats to include in each of the tests; each test included over 60 samples. The approach that was developed involved the use of an aluminum oxide ceramic platform (D-Tube), on which the samples were oriented using machined aluminum oxide ceramic sample holders. Samples were oriented within the holders using machined notches spaced along their length. In the case of the thicker samples (PS400) and cylindrical samples, these were placed directly onto

the ceramic platform rather than in a machined sample holder. The photos in Figure 7 show how the holder was utilized for the curved foil (A) and flat foil (B) samples, while the photo in Figure 8 shows how the holder was utilized for the full suite of samples in a single test. The dimensions for the holder were 13" long and 1.5" wide, and the height was such that the samples were positioned at the vertical center of the furnace.



Figure 6. Modified autoclave furnace for gas foil bearing tests at 300psi CO₂

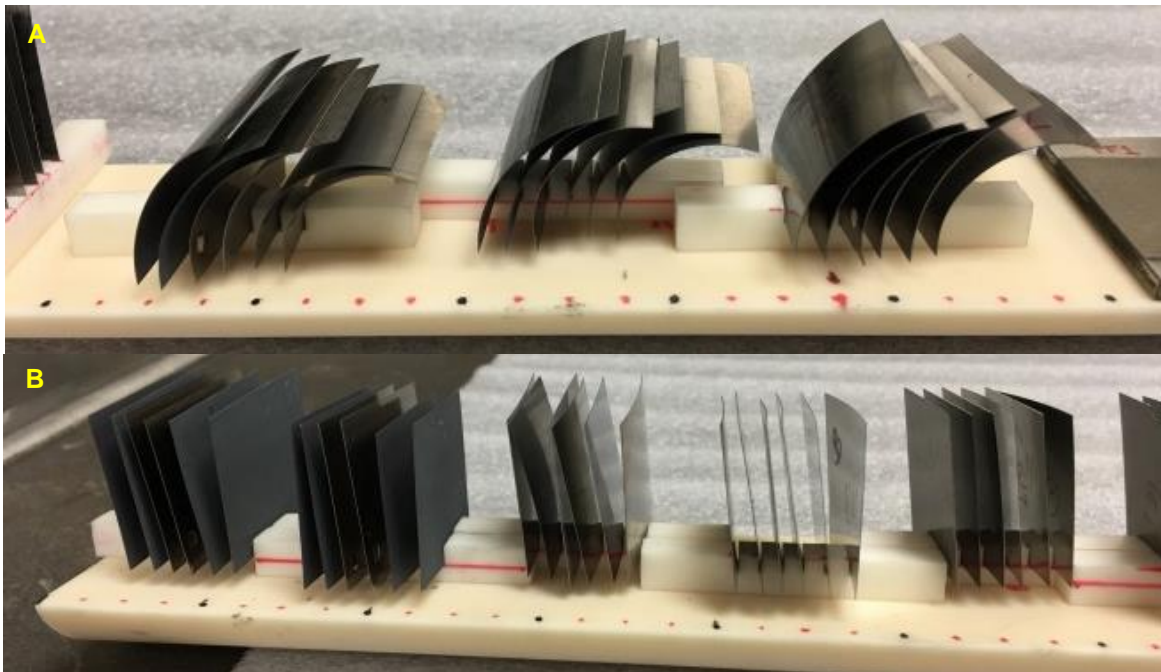


Figure 7. Sample holder configuration used for curved foil samples (A) and flat foil samples (B)



Figure 8. Sample holder loaded up with the full complement of samples for an exposure test

Two long duration exposure experiments were performed using this setup, covering the two exposure conditions relevant to bearing foil materials. In one test, an exposure temperature of 550°C was used to mimic the conditions for the turbine-side journal bearings. In a second test, a temperature of 315°C was used to mimic the conditions for the compressor-side journal and thrust bearings. In each test, the total exposure duration was 500 hours, which is significantly longer than has been achieved previously for bearing foil materials in these environments. Industrial grade CO₂ was used for both experiments in order to mimic the conditions inside of a bearing that would be used in a real system.

Four samples of each coating material and sample format were included into each of these exposure experiments. This was done to be able to provide samples for the various post-test analyses that are described in the next section of this paper. Also, having multiple samples of each coating material/sample format adds reliability to the data from these experiments instead of basing all of the analyses / results off of a single sample. Information for each of the coating materials investigated through this set of experiments are summarized in Table 1. Pertinent information for the materials from both Xdot and Mechanical Solutions are included, along with the available information for the “baseline” bearing materials currently used in the Sandia RCBC system.

Table 1. Descriptions of Bearing Foil Coating Materials

Sample Name	Bearing Vendor	Coating Vendor	Coating Name	Coating Mtl	Coating Thickness (microns)	Substrate Alloy	Turbine, Compressor, Both
MoS ₂	Xdot	Everlube	Perma-slik RMAC	MoS ₂	10-16	X750 Inconel	Both
WS ₂	Xdot	Everlube	Perma-slik RWAC	WS ₂	30	X750 Inconel	Both
10K2	Xdot	General Magnaplate	Nedox 10K2	Ni-P and Si-O	7-8	X750 Inconel	Turbine
10K3	Xdot	General Magnaplate	Nedox 10K3	Ni-P and Si-O	13-23	X750 Inconel	Compressor
TC A	Xdot	TurboCAM	TX1 (Treatment A)	Nitride Surface Treatment	n/a	316 ss	Both
TC B	Xdot	TurboCAM	TX1 (Treatment B)	Nitride Surface Treatment	n/a	316 ss	Both
TC C	Xdot	TurboCAM	TX1 (Treatment C)	Nitride Surface Treatment	n/a	316 ss	Both
PS400	Xdot	Hohman Plating (NASA)	PS400	NiMoAl, Cr-oxide, Ag, Ba-Ca fluorides	380-500	15-5 ss	Both
A39	Mechanical Solutions	Mechanical Solutions	A39	n/a	1.50	X750 Inconel	Both
A40	Mechanical Solutions	Mechanical Solutions	A40	n/a	1.50	X750 Inconel	Both
A42	Mechanical Solutions	Mechanical Solutions	A42	n/a	1.50	X750 Inconel	Both
Baseline-Thrust	SNL	Barber-Nichols Inc.	Unknown	Teflon	20-22	X750 Inconel	Compressor
Baseline-Journal (LT)	SNL	Capstone Turbines	Unknown	Teflon	n/a	X750 Inconel	Compressor
Baseline-Journal (HT)	SNL	Capstone Turbines	Unknown	Unknown	n/a	X750 Inconel	Turbine

3.3. Test Sample Characterization

The approach to sample characterization was focused around understanding the chemical compatibility of the materials with its environment, and how these interactions may influence the materials performance as a bearing foil coating. Conversely, understanding and characterizing the tribological properties of the coating materials in their use environments was not the focus. Through discussions with the participant bearing vendors, it was determined that the tribological performance for these materials would be best characterized through start-stop testing in the future bearing-test rig, as these properties need to be measured as the material is being used in its intended environment. Along this vein, the characterizations identified for these exposure tests were intended as a screening tool to identify candidate coating materials for further evaluations in the bearing-test rig.

The main areas of sample characterization included in this investigation included microscopic examination of the coating/substrate microstructure, surface roughness measurements, and scratch testing to reveal a variety of parameters around the durability of the coating material. These areas were determined through conversations with subject matter experts internal to Sandia as well as those external (NASA, Xdot, and Mechanical Solutions). Details are provided for each of these areas of sample characterization in the following sections.

3.3.1. Coating/Substrate Microstructure

Environmental exposure of the samples can cause microstructural changes to the coating material itself or to the coating/substrate interface. These are important to characterize and understand for each of the candidate coating materials. Microstructural changes of the coating material can contribute to changes in other sample characteristics such as surface roughness, damage resistance, and adhesion strength to the substrate. Changes to the coating/substrate interface, possibly caused by oxidation reactions with the CO₂ environment, can influence the coating adhesion strength to the substrate.

For each sample type, one specimen was characterized for microstructural changes. This was done for samples in the pre-exposed condition, as well as for after each of the two exposure conditions, so that comparisons could be made among the three conditions (no exposure, 500hrs at 550°C, and 500hrs at 315°C). Samples were prepared for analysis by mounting in epoxy, cross-sectioning, polishing, and applying a thin gold coating by sputter deposition. Prepared samples were analyzed using a JEOL JSM-7600F field emission scanning electron microscope (SEM) together with an Oxford Instruments X-Max 80mm² detector for Energy Dispersive Spectroscopy (EDS).

3.3.2. Surface Roughness

The surface roughness for bearing foils can have a strong influence over their performance in a bearing. In general, lower surface roughness is desirable over a higher roughness. Also, it is desirable to avoid large surface roughness increases following exposure of the bearing foil coating to its use environment. So, for each of the bearing coating materials, it is important to characterize the changes that result during the 500 hour environmental exposures.

Surface roughness measurements were completed for two flat foil samples of each type. Measurements were completed for samples prior to exposure, followed by repeat measurements on the same exact samples following the completion of the exposure experiments. Three measurements were made in different areas on each sample. Measurements were completed using a Keyence VK-X Series 3D Laser Scanning Confocal Microscope, which provides non-contact, nanometer-level profile and roughness measurements.

A range of output data, relating to the sample surface roughness, is provided from these measurements. Three separate images are provided of the sample surface, in addition to a range of surface roughness parameters. The images are useful for comparing among the different coating materials, as well as for a single sample to understand the changes that occur following environmental exposure. Regarding the surface roughness parameters, the most useful value is the arithmetical mean height (S_a), as it expresses the difference in height of each point compared the arithmetical mean of the surface. Lower values for S_a are indicative of smoother surfaces with lower surface roughness.

3.3.3. Scratch Testing

The scratch resistance and adhesion strength of coating materials can be determined using the instrumented scratch testing method. In evaluating bearing foil coating materials these are important

parameters to understand between the various coatings as well as for the same material as a function of environmental exposure. The foil coating material should be resistant to damage (scratching, etc.) and have strong adherence to the metal substrate; both are important to avoiding debris generation within the bearing as well as maintaining the low friction coating surface for periods of operation where rubbing occurs.

In this test method, a diamond stylus of defined geometry is drawn across the flat surface of a coated test specimen at a constant speed and defined normal force (progressively increasing) for a defined distance. The damage along the scratch track is microscopically assessed as a function of the applied force. This technique is able to differentiate between cohesive failure within the coating (coating scratch damage resistance) and adhesive failure at the interface of the coating-substrate system (coating adhesion strength).

This test method is illustrated in Figure 9. Here, several pieces of information are brought together to demonstrate the method. The drawing at the top illustrates the damage that occurs to the coating material as the stylus moves across the surface. The two types of coating failure, cohesive and adhesive, are indicated here. Below this is a microscopic image of the sample surface. Again, the two distinct types of coating failure are indicated. The visual differences between these types of failure are used to indicate when these occur for a test sample. Finally, at the bottom is a chart indicating the applied normal force (blue), the resulting frictional force (green) and stylus penetration depth (red) across the length of the scratch. The microscopic image together with the chart are used to identify the force at which the two types of failure occur for a sample.

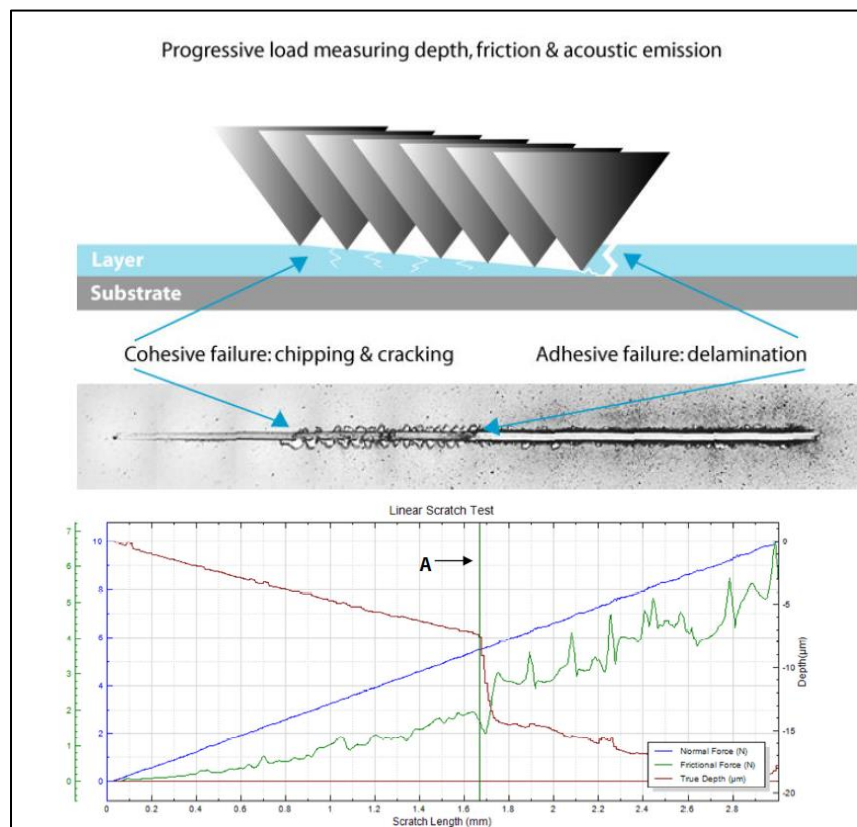


Figure 9. Illustration of multiple elements to instrumented scratch testing

Flat foil samples of each type for each environmental exposure condition were sent out to EP Laboratories

in Irvine, California for instrumented scratch testing. Unexposed flat foil samples of each type were also sent for testing. Testing was completed in triplicate for each sample, and followed the relevant ASTM Standards (G171, C1624, and D7187). The test conditions and parameters used for tests are provided in Table 2.

Table 2. Test Conditions and Parameters used for Instrumented Scratch Testing

Load Type	Progressive
Initial Load	3 mN
Final Load	500 mN
Scanning Load	3 mN
Loading Rate	500 mN/min
Scratch Length	1 mm
Speed	1 mm/min
Distance between scratches	1 mm
Cantilever	HL-125
Indenter	Rockwell Diamond Radius 10 μm ID: SD-A33/90
Indenter Source	CSM Instruments
Indenter Inspection	Indentation in Copper Before and after testing samples
Temperature	21-23°C
Relative Humidity	45-48%
Conditioning	21-23°C for minimum 24h

4. RESULTS

Sample characterization included microscopic examination of the coating/substrate microstructure, surface roughness measurements, and scratch testing to reveal a variety of parameters around the durability of the coating material. Results are presented for coating materials in each of these areas for the two separate 500 hour exposure experiments.

4.1. Coating/Substrate Microstructure

SEM cross-sections of each of the sample types are compared for the three relevant conditions: Non-exposed, 315°C exposure, and 550°C exposure. These are shown for each of the samples in the flat format in Figure 10 and Figure 11. The plan was to also to examine cross-section microstructures for the curved foil samples, but these were not completed due to time constraints. All of these samples are available for future analysis if needed.

The most notable general observation for all of these samples, is that the lower temperature exposure resulted in relatively minor microstructural changes, while the higher temperature resulted in rather dramatic changes for many of the materials. An exception to this was the baseline thrust bearing foil sample which was observed to be severely degraded by the lower temperature exposure. Another exception was for both the MoS₂ and WS₂ samples, which didn't exhibit significant microstructural change at either exposure temperature.

Some samples exhibited extensive microstructural damage, which may preclude them from future consideration/testing as a bearing foil coating material. For the 315°C environment, the analysis suggests that the TX1 samples be eliminated from consideration. Chemical analysis of the corrosion products on the TX1 material is shown in Figure 12. While the nitrogen is still found near the surface and may be able to impart the desired hardness and wear resistance, an iron-based oxide is found on the surface that could spall and contribute to particulate generation within the bearing. The baseline thrust bearing coating also exhibited severe microstructural damage at the lower temperature. This may be attributable to a testing temperature above that which the bearing actually sees, since the degradation observed in this test was much more severe than is typically observed for these bearings. Nonetheless, it is good to know that other bearing coating materials are available that can tolerate this 315°C exposure temperature without the same degradation.

For the 550°C environment, several of the samples could be eliminated from consideration based on the severity of the microstructural damage observed. The TX1 sample oxidation, that was a problem at the lower temperature, was even more problematic at this higher temperature. Chemical analysis of the corrosion products on this sample are shown in Figure 13. The oxide is now much thicker and consists of an inner chrome-oxide layer and outer iron-oxide layer. Severe oxide spallation was observed from the curved samples with this coating at this higher temperature, which is shown in Figure 14. This material should be eliminated from consideration in bearing foils at both of the exposure conditions. Also, the 10K2 coating is not recommended for use at this temperature due to coating delamination from the foil substrate. Chemical analysis of this coating is shown in Figure 15. The substrate surface was observed to be depleted in chromium, as a precipitated Cr-S phase was found within the Ni-P coating layer. This may have contributed to the coating delamination that was observed. Also, islands of a Ni-S phase were found on top of the coating surface, which may contribute to increased surface roughness.

Microstructural degradation was observed for both the PS400 as well as the Mechanical Solutions samples (A39, A40, A42) at the higher temperature, but neither should be precluded from future consideration based on this. In the case of the PS400, the coating material itself did not change. Instead, oxidation was observed to occur at the coating-substrate interface. A chemical analysis of the coating-substrate interface is provided in Figure 16, which shows the formation of iron-oxide at the interface. This is partially attributable to the substrate material, rather than to the coating. The PS400 was applied to a 15-5 stainless steel substrate, which is significantly more susceptible to corrosion in CO₂ environments than for the Inconel X750 substrates used with many of the other coatings. One could argue that the MoS₂ or WS₂ samples, which also did not exhibit obvious degradation of the coating material, would have demonstrated similar substrate oxidation as the PS400 if they had been put down on the 15-5 alloy rather than X750.

In the case of the three Mechanical Solutions coatings, they all appear to change following the high temperature exposure. It appears that the coating material either reacts with the substrate alloy or there is internal oxidation that occurs below the surface of the substrate. The coating material itself appears to remain intact and may indeed function well as a bearing coating. Due to the NDA that is established with them, the authors are unable to provide any additional information regarding the chemistry of the coating itself or any of the reaction products.

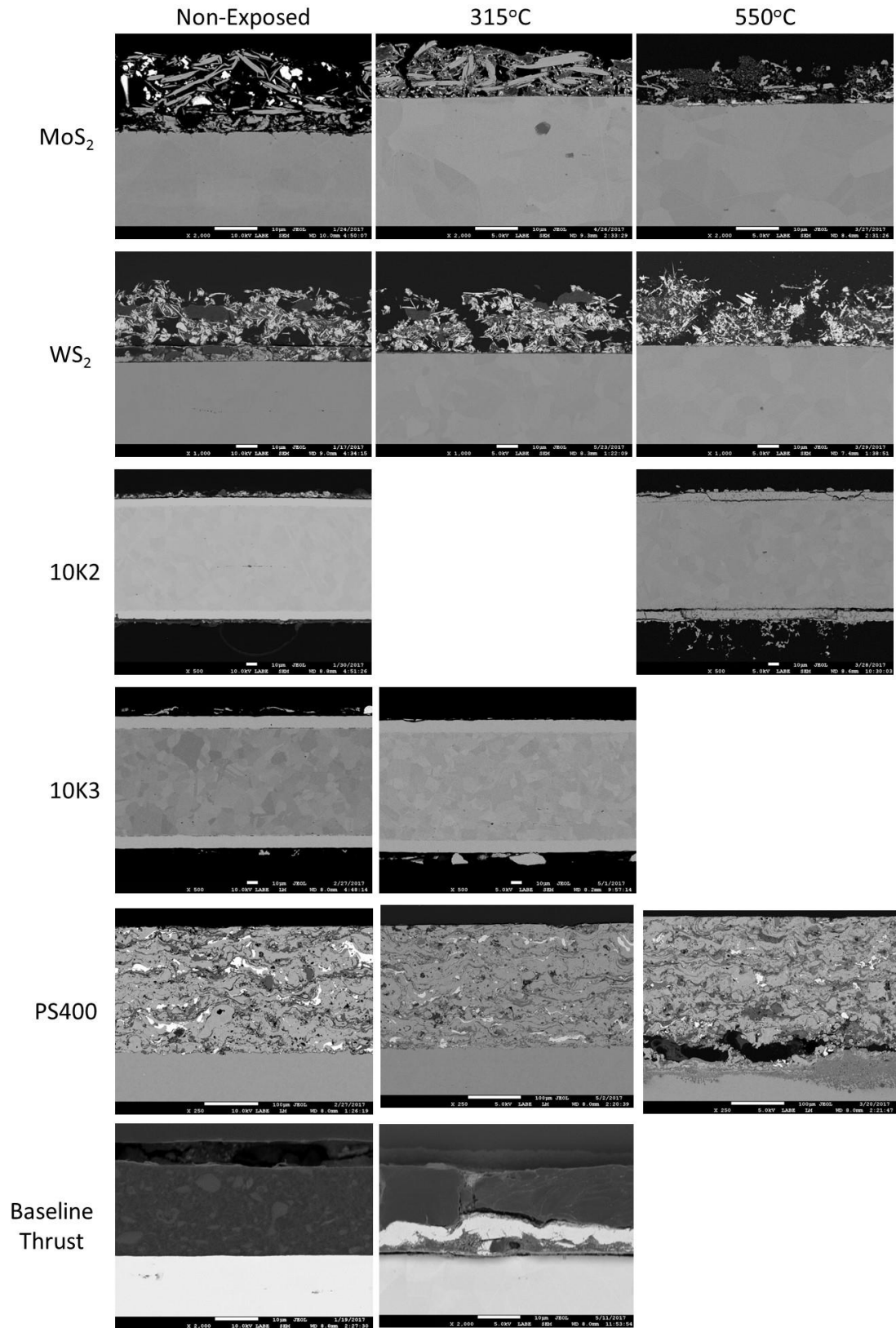


Figure 10. SEM cross-sections for one set of samples compared for the three conditions

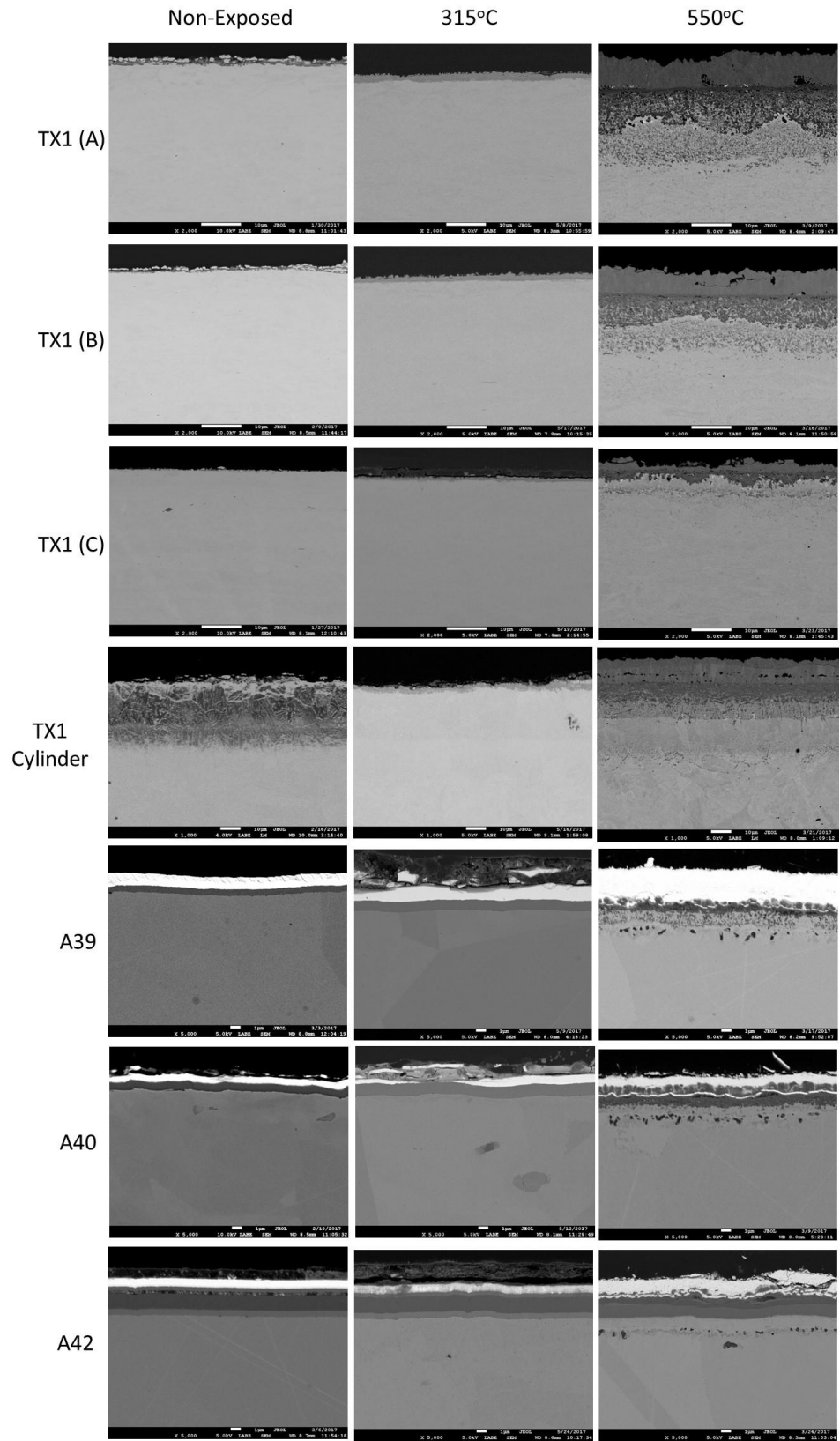


Figure 11. SEM cross-sections for a second set of samples compared for the three conditions

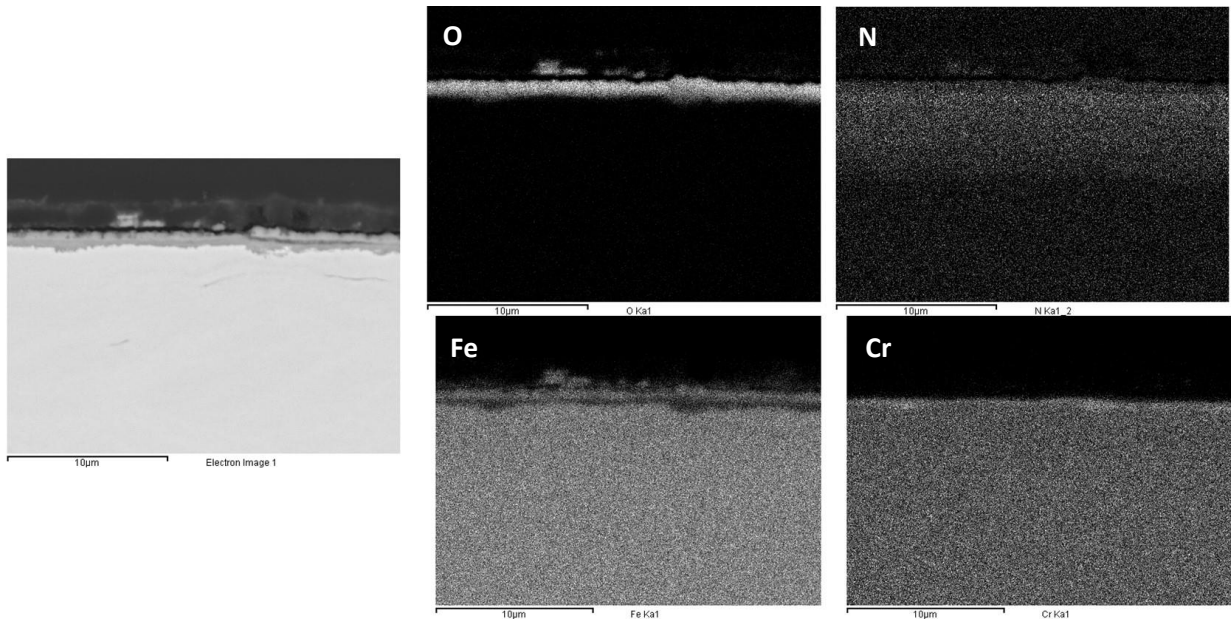


Figure 12. EDS chemical analysis for the TX1 coating exposed at 315°C

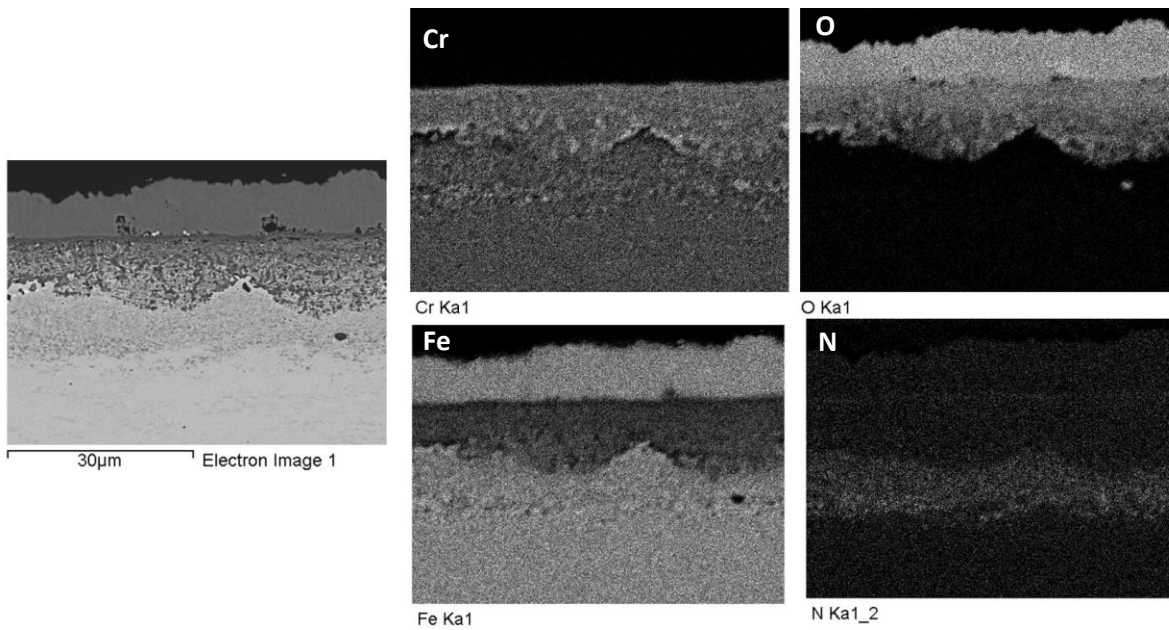


Figure 13. EDS chemical analysis for the TX1 coating exposed at 550°C



Figure 14. Oxide scale spallation for the TX1 coating exposed at 550°C

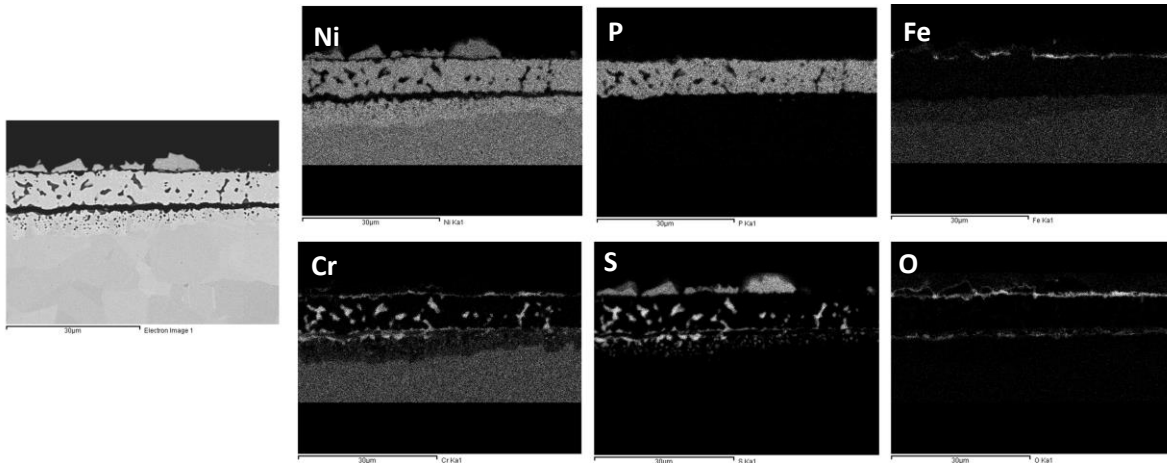


Figure 15. EDS chemical analysis for the 10K2 coating exposed at 550°C

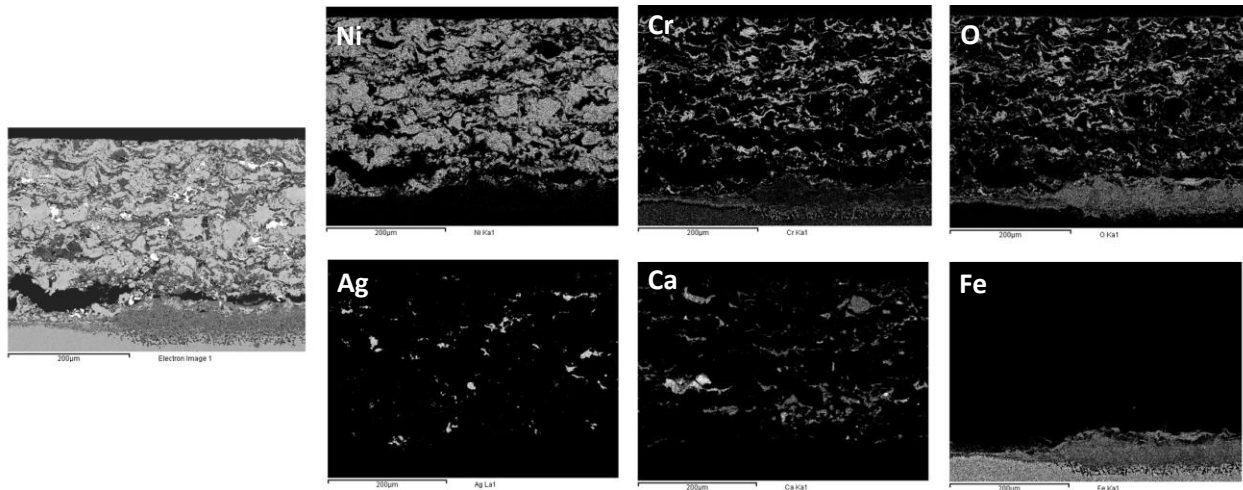


Figure 16. EDS chemical analysis for the PS400 coating exposed at 550°C

4.2. Surface Roughness

The surface roughness for samples are evaluated as a means of assessing how the various coating materials may be expected to perform in a bearing during rubbing. While it is only one variable of many that may contribute to its performance, a lower surface roughness is expected to improve bearing performance. It is useful to compare samples amongst themselves, but also to evaluate how sample roughness changes as a result of exposure to the high temperature, high pressure CO₂ environments.

Surface roughness values for the samples in the 315°C experiment are shown in Figure 17. The samples with the highest roughness are those with the MoS₂ and WS₂ coatings. The other coating materials are comparable to each other, without significant differences. In general, the changes in surface roughness with the exposure environment were small, and generally decreased. An exception to this is the PS400 material which exhibited a large drop in surface roughness after exposure. In fact, it exhibited the lowest post-exposure surface roughness for any of the samples.

Surface roughness values for the samples in the 550°C experiment are shown in Figure 18. Again, the MoS₂ and WS₂ samples are identified as having the highest surface roughness. Also, both materials are observed to have increasing surface roughness following the environmental exposure. In fact, most of

the candidate materials exhibited increased surface roughness following the exposure, and the surface roughness values are higher than those from the lower temperature exposure. It is unclear what contributes to these trends, but future bearing-rig tests should be valuable to explore this in more depth.

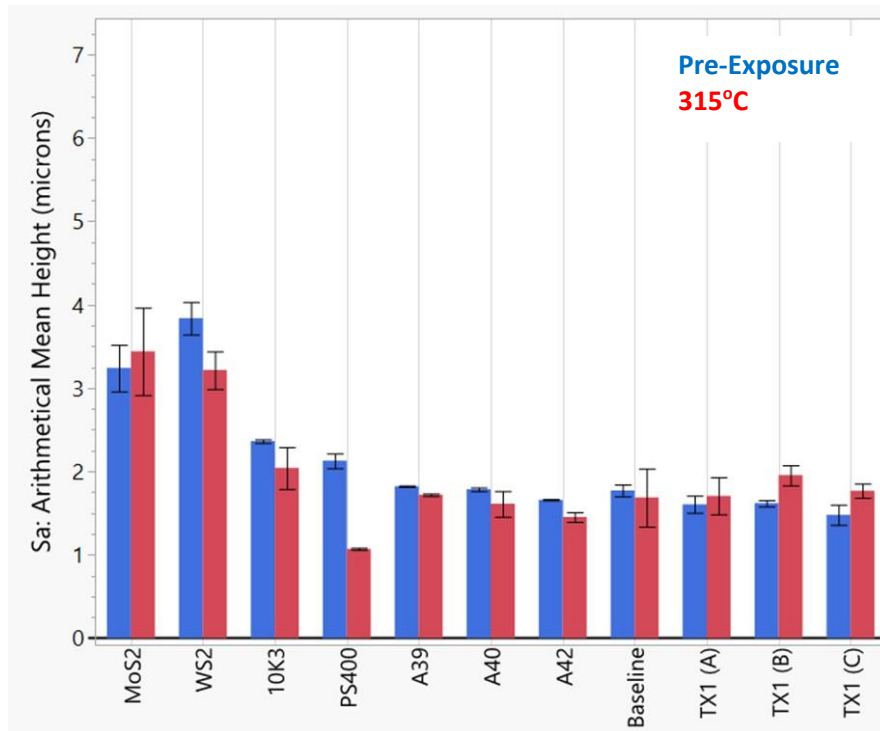


Figure 17. Surface roughness measurements for the 315°C exposure test samples

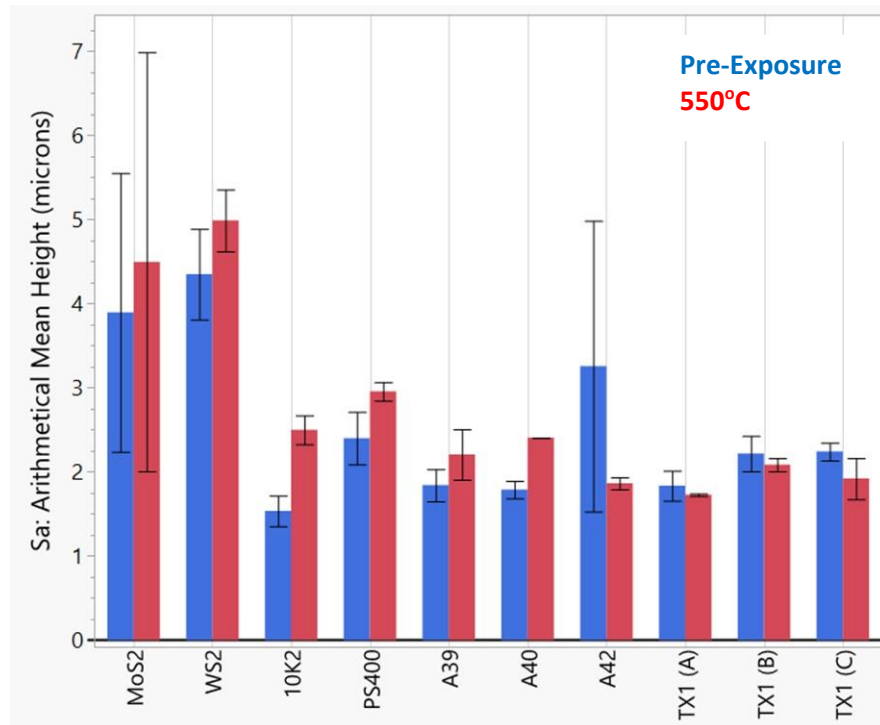


Figure 18. Surface roughness measurements for the 550°C exposure test samples

4.3. Scratch Testing

The two pieces of information obtained from the instrumented scratch testing are (1) the force at which coating cohesive failure occurs, and (2) the force at which coating adhesive failure occurs. The first relates to the ease with which the coating is able to be scratched or damaged, while the second relates to how strongly adhered the coating is to the substrate. Both are valuable metrics to consider in selecting bearing foil coating materials. High force values for both types of failure are desirable over low values.

The measured values for cohesive failure are provided for all of the coating materials at each of the test conditions (Pre-exposure, 315°C, and 550°C) in Figure 19. The WS₂ and Baseline thrust bearing coatings were the easiest to damage, and neither changed much with the environmental exposures. A legitimate concern for these samples would be the easy removal of the coating material from the bearing during rubbing. Some samples exhibited high damage resistance prior to exposure, but significantly lower resistance after exposures. This is particularly true for the MoS₂ and the three Mechanical Solution coatings (A39, A40, A42). For these samples, the changes in damage resistance were modest at the 315°C exposure, but decreased significantly at the 550°C exposure. For other samples, the damage resistance was low initially, but showed significant increase after environmental exposure. Obviously, this is preferable to the opposite scenario. This was observed for the 10K2, 10K3, and PS400 samples.

Measured values for adhesive failure are provided for the same coating materials at the same three test conditions in Figure 20. Similarly, to the cohesive failure values, two divergent trends are observed. For some of the samples, the coating adhesion was largest pre-exposure, and decreased with the environmental exposures. This was observed for the three Mechanical Solutions samples (A39, A40, A42), the Baseline thrust bearing coating, and the TX1 samples. Most dramatic among these were the Mechanical Solutions and Baseline samples. These started out with the best coating adhesion strengths, but dropped to some of the lowest values of any following the exposures. For the Mechanical Solutions coatings, the adhesion strengths were higher than any of the other materials following the 315°C exposure, but were some of the lowest values following the 550°C exposure. Samples exhibiting the opposite trend of increasing coating adhesion strength with environmental exposure, were the MoS₂, WS₂, 10K2, 10K3, and PS400 samples.

To summarize, the samples with the highest pre-exposure damage resistance were the Mechanical Solutions samples. These same samples also had the highest damage resistance after the 315°C exposure, while the sample with the highest damage resistance after the 550°C exposure were the PS400 sample. The samples with the highest pre-exposure adhesion strength were the Mechanical Solutions samples and the Baseline thrust bearing sample. Those with highest strength after the 315°C exposure were the Mechanical Solutions samples, and after the 550°C exposure were the MoS₂, WS₂, and PS400 samples.

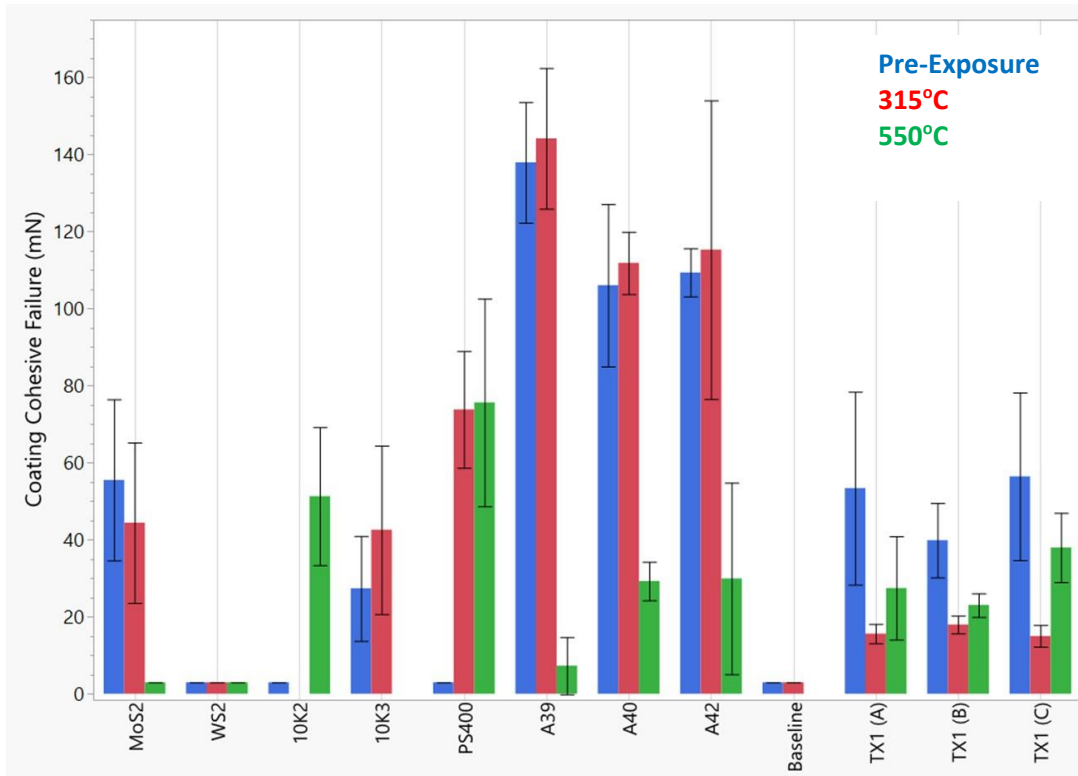


Figure 19. Measured cohesive failure values for each coating material at all exposure conditions

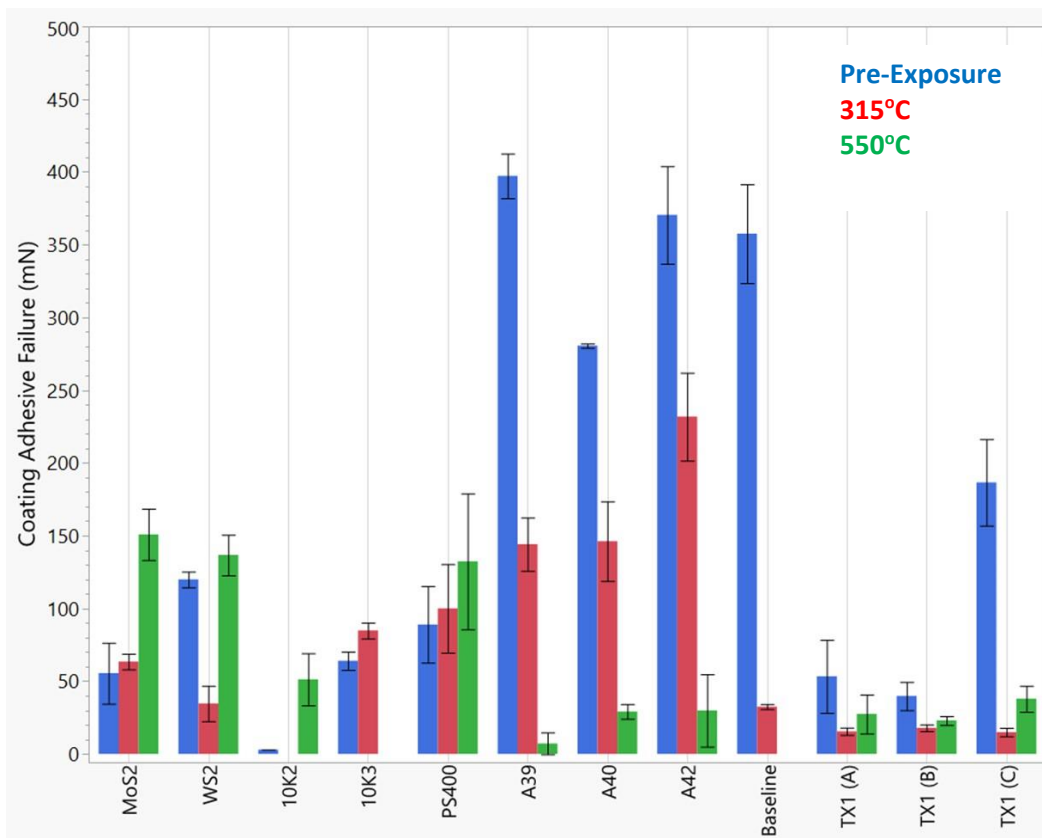


Figure 20. Measured adhesive failure values for each coating material at all exposure conditions

5. SUMMARY

A need was identified for evaluating gas foil bearing coating materials in environments relevant to S-CO₂ power systems. In response to this need, a test configuration was developed enabling long duration exposure tests, followed by a range of analyses relevant to their performance in a bearing. Analysis by members of the Sandia S-CO₂ team in Albuquerque, NM established a pressure of 300 psi CO₂ at both the turbine-side and compressor-side bearings. Additionally, a temperature of 550°C was established for the turbine-side bearings, and a temperature of 315°C was established for the compressor-side. Long duration (500 hours) experiments at both conditions, provide valuable data regarding the performance of bearing coating materials in these environments. This paper provides a detailed overview of this work, which involved significant collaboration with industrial gas foil bearing vendors. The results contained herein provide valuable information in selecting appropriate coatings for more advanced future bearing-rig tests at the newly established test facility in Sandia-NM as well as in other facilities that may exist for these types of tests.

Sample performance was assessed across several different areas following environmental exposures. These included coating/substrate microstructure, surface roughness, and scratch testing. Based on these analyses, a series of recommendations are made for materials to include in future bearing-rig tests.

The TX1 coating materials performed poorly in many of the categories and should be eliminated from future consideration. The most prominent problem with these are their associated surface oxidation, which would lead to particulate generation within the bearing. The baseline thrust bearing coating (Teflon-based) also performed poorly across several categories. It is easily damaged both before and after environmental exposure, and the coating adhesion strength is significantly reduced following the 315°C exposure. Significant cracking/peeling of the coating along the foil surface was also observed. These are not observed for this material following operation in the Sandia RCBC, and so it is possible that 315°C is a higher temperature than the thrust bearing truly experiences. Conversely, it is possible that it does see this temperature in the RCBC, but that the short duration exposures don't reveal the degradation that this long duration exposure has revealed. A third material that should be eliminated from consideration is the 10K2 Nickel based coating. This material, being considered for only the higher temperature environment, exhibited significant delamination from the substrate following the exposure test.

Each of the other coating materials (10K3, MoS₂, WS₂, PS400, and the three Mechanical Solutions materials) are recommended for additional performance evaluations as bearing coating materials. The 10K3 material, being considered for only the 315°C condition, performed well in all areas of testing. The MoS₂ and WS₂ coatings, appeared to be very stable in the exposure environments, and together with the PS400 material, had the highest coating adhesion strength after the 550°C exposure. On the negative side, they had the highest surface roughness and very low damage resistance following the 550°C exposure. The PS400 material was very stable in the environments, had the best post-exposure damage resistance in both environments, and had very high coating adhesion strength following both exposures. It also exhibited the lowest surface roughness after the 315°C exposure. As a negative, substrate oxidation was observed for the 550°C exposure, but the change to the 15-5 stainless steel alloy here in place of the Inconel X750 substrate used for the foil samples, certainly played a role. Finally, the three Mechanical Solutions materials exhibited good surface roughness, had the highest damage resistance and substrate adhesion strength as pre-exposed and 315°C exposed. For the 550°C exposure they didn't perform so well in these two areas. A reaction is believed to occur between the coating material and substrate at this higher temperature, and this may be contributing.

NOMENCLATURE

S-CO₂ = Supercritical Carbon Dioxide
US DOE-NE = United States Department of Energy – Nuclear Energy Division
RCBC = Recompression Closed Brayton Cycle
OEM = Original Equipment Manufacturer
TAC = Turbine-Alternator-Compressor
SEM = Scanning Electron Microscope
EDS = Energy Dispersive Spectroscopy

ACKNOWLEDGEMENTS

Sandia National Laboratories is a multimission laboratory managed and operated by National Technology & Engineering Solutions of Sandia, LLC, a wholly owned subsidiary of Honeywell International, Inc., for the U.S. Department of Energy's National Nuclear Security Administration under contract DE-NA0003525. Special acknowledgements to Ken Stewart for his contributions to this work through the modification and setup of the autoclave furnace used for these experiments. Also, I would like to acknowledge Jeff Chames and Andy Gardea for their valuable contributions through microscopy sample preparation and analysis. Adriana Panders is also acknowledged for her contributions to the surface roughness measurements.

REFERENCES

1. McHugh, J.D. (1979). Principles of Turbomachinery Bearings. In: Proceedings of the 8th Turbomachinery Symposium, Texas A&M University, 135-144.
2. Brun, K., et al. (2017). *Fundamentals and Applications of Supercritical Carbon Dioxide (SCO₂) Based Power Cycles*. Woodhead Publishing.
3. Chapman, P.A. (2016). Advanced gas foil bearing design for supercritical CO₂ power cycles. In: The 5th International Symposium - Supercritical CO₂ Power Cycles, San Antonio, Texas.
4. Ahn, Y., et al. (2015). Review of Supercritical CO₂ Power Cycle Technology and Current Status of Research and Development, Nuclear Engineering Technology (47), 647-661.
5. Cho, J., et al. (2016). Research on the Development of a Small-Scale Supercritical Carbon Dioxide Power Cycle Experimental Test Loop. In: Proceedings of the 5th International Symposium – Supercritical CO₂ Power Cycles, March 28-31, San Antonio, Texas.
6. Preuss, J.L. (2016). Application of hydrostatic bearings in supercritical CO₂ turbomachinery. In: Proceedings of the 5th International Symposium – Supercritical CO₂ Power Cycles, March 28-31, San Antonio, Texas.
7. Devitt, D. (2016). Porous externally pressurized gas bearings. In: Proceedings of the 5th International Symposium - Supercritical CO₂ Power Cycles, March 29 - 31, San Antonio, Texas.
8. Conboy, T. (2012). Gas Bearings and Seals Development for Supercritical CO₂ Turbomachinery, Sandia Report: SAND2012-8895.
9. DellaCorte, C., Edmonds, B. (2009). NASA PS400: A New High Temperature Solid Lubricant Coating for High Temperature Wear Applications, NASA Report: 2009-215678.
10. DellaCorte, C., et al (2010). The Effect of Composition on the Surface Finish of PS400: A New High Temperature Solid Lubricant Coating, NASA Report: 2010-216774.
11. Walker, M., et al (2016). Progress in Overcoming Materials Challenges with S-CO₂ RCBCs: Final Report, Sandia Report: SAND2016-9774.